XXIV Reunión Nacional y VIII Congreso Ibérico de ESPECTROSCOPIA

ABSTRACT BOOK

XXIV RNE – VIII CIE
ESPECTROSCOPIA

Logroño, 9-11 de julio de 2014

COMUNICACIONES TIPO PÓSTER

SESIÓN DE CARTELES 1

Alimentos. Análisis bioquímico. Especiación. Análisis forense. Medio ambiente, Patrimonio histórico. Sensores.

P001 Stability assessment of virgin olive oils enriched with new natural antioxidants using spectrophotometric colour monitorization. *R. Bermejo, P. Limón, A. Navarro, A. Ortiz, M. P. Fernández-Liencres, F.G. Acién-Fernández, J.M. Fernández-Sevilla and M. Melgosa.*

P002 Multielemental analysis of plant samples by total reflection X-ray fluorescence together with linear discriminant analysis to identify the anatomical part. *C. Bendicho, I. De la Calle, M. Costas, V. Romero, I. Costas, I. Lavilla.*

P003 Classification of Spanish red wines according to their designation of origin using laser–induced breakdown spectroscopy and neural networks. *S. Moncayo, E. Stamati, E. Sánchez–Tirado, J.D. Rosales, J.O. Cáceres.*

P004 Determination of resveratrol, piceatannol and oxyresveratrol isomers in wines using stir bar sorptive extraction and gas chromatography-mass spectrometry. *J.I. Cacho, N. Campillo, P. Viñas and M. Hernández-Córdoba.*

P005 Development of multivariate models for quantifying microbial load in goat milk by near infrared spectroscopy. *F. Cámara-Martos, P Krepelka, G.D. Posada-Izquierdo, F. Pérez-Rodríguez.*

P006 Spectroscopical study of compounds emitted by household ovens. *A. Delgado-Camón, S. de Marcos, J. Sanz, J. Galbán.*

P007 Migration and characterization of nanosilver particles from food containers by AF4-ICP-MS. *G. Artiaga, K. Ramos, L. Ramos, C. Cámara, M. Gómez-Gómez.*

P008 Direct determination of essential elements in food and dietary supplements by high-resolution continuum source atomic absorption spectrometry. *B.Gómez-Nieto, Mª J. Gismera, Mª T. Sevilla, J.R. Procopio.*

P009 Determination of caffeoylquinic acids in feed and related products by focused ultrasound solid-liquid extraction and ultra-high performance liquid chromatography-mass spectrometry. *M.T. Tena, M. P. Martínez-Moral, P. W. Cardozo.*

P010 Using spectroscopy vis/NIR to determinate quality parameters in *Prunus avium* "Chelan" sweet cherries. *A. I. Negueruela, V. Lafuente, J. Val.*

P011 Cloud point extraction with silver nanoparticles for the determination of very low amounts of cadmium by electrothermal atomic absorption spectrometry. *I. López García, Y. Vicente-Martínez, M. Hernández-Córdoba.*

P012 Determination of lead in wine samples by means of dispersive liquid-liquid microextraction and graphite furnace atomic absorption detection. *D. Martínez, G. Grindlay, L. Gras, J. Mora.*

P013 A novel method for evaluating flavanols in grape seeds by near infrared hyperspectral imaging. *F. J. Rodríguez‑Pulido, J. M. Hernández-Hierro, J. Nogales-Bueno, B. Gordillo, M. L. González-Miret, F. J. Heredia.*

P014 Application of the characteristic vector method to the reconstitution of red grape NIR spectra. *J. Nogales-Bueno, F. Ayala, J. M. Hernández-Hierro, F. J. Rodríguez-Pulido, J. F. Echavarri, F. J. Heredia.*

P015 Feasibility study on the use of near infrared hyperspectral imaging for the screening of anthocyanins in intact grapes during ripening. *J. M. Hernández-Hierro, J. Nogales-Bueno, F. J. Rodríguez-Pulido, F. J. Heredia.*

P016 Determination of the geographical origin of cocoa beans by means spectrometric methods and chemometrics. *D. Lledó, G. Grindlay, L. Gras, J. Mora.*

P017 Time-course evolution of catechin, gallic acid and resveratrol in vinification process by ^{1}H NMR spectroscopy. *E. López-Rituerto, A. Avenoza, J.H. Busto, J.M. Peregrina.*

P018 Neurotransmitters determination based on the auto-indicating properties of enzymes. *S. de Marcos, J. Navarro, E. Ortega-Castell, J. Galbán.*

P019 Impact of a dietary antioxidant in cancer cells: a Raman microspectroscopy study. *J. Monteiro, A.L.M. Batista de Carvalho, L.A.E. Batista de Carvalho, M.P.M. Marques.*

P020 Determination of biochemical parameters in human serum by near-infrared spectroscopy. *S. Garrigues, J. L. García-García, D. Pérez-Guaita, J. Ventura-Gayete, M. de la Guardia.*

P021 Bioavailability, bioaccessibility and speciation of as and other heavy metal elements in contaminated areas of Chile. *I. Pizarro, D. Román, M. Gómez y M.A. Palacios.*

P022 Troubleshooting in arsenic species analysis in human urine by high-performance liquid chromatography inductively coupled plasma-mass spectrometry. *Jorge Moreda-Piñeiro, Alicia Cantarero-Roldán, Paloma Hermelo-Herbello, Antonio Moreda-Piñeiro, Pilar Bermejo-Barrera.*

P023 Determination of thiametoxam by a multicommutated flow-through optosensor based on photochemically induced fluorescence. *A. Ruiz-Medina, J. Jiménez-López, P. Ortega-Barrales.*

P024 Identification and discrimination of bones remains by laser inducted breakdown spectroscopy and neuronal networks. *L. Ugena García-Consuegra, S. Moncayo, S. Manzoor, R.C. Izquierdo- Hornillos, F.J. Manuel de Villena, J.O. Cáceres.*

P025 Deeping on analysis of glass samples by LA-ICP-MS for forensic pairwise comparisons. *M. Calcerrada, F. Alamilla, C. García-Ruiz, M. Torre.*

P026 Synthesis, characterization and application of Mn-doped ZnS quantum dot – molecularly imprinted polymers for fluorescence detection of cocaine and analogues in urine. *María del Pilar Chantada-Vázquez, Juan Sánchez-González, Elena Peña-Vázquez, Ana María Bermejo, María José Tabernero, Pilar Bermejo–Barrera, Antonio Moreda–Piñeiro.*

P027 Novel electrospinning-produced turn-on fluorescence microfibre mat encapsulating a Rhodamine 6G derivative for Hg^{2+} determination in water samples. *A. Muñoz de la Peña, F.J. Orriach-Fernández, A. L. Medina-Castillo, J. F. Fernández-Sánchez, A. Fernández-Gutierrez.*

P028 use of microextraction by packed sorbents in the determination of brominated flame retardants in sewage sludge. *M.P. Martínez-Moral, M.T. Tena*.

P029 dissolution of natural scorodite in a waste pile and its role as arsenic carrier evaluated by EXAFS, TEM and single particle - ICPMS detection. *M.A. Gomez-Gonzalez, F. Laborda, F. Garrido, P. O'Day, E. Bolea, J.R. Castillo*.

P030 Evaluation of a simple and fast method for on-line preconcentration of trace elements by ICP-MS. *M.C Barciela Alonso, N. Adega Rivas, E. Peña Vázquez, P. Bermejo-Barrera*.

P031 Identification of harmful compounds present in steel slag used in forest tracks through spectroscopic techniques*. L. Gomez-Nubla, J. Aramendia, S. Fdez.-Ortiz de Vallejuelo, J. M. Madariaga.*

P032 Application of a molecularly imprinted polymer for mercury preconcentration in water samples. *R. Rodríguez-Fernández, E. Peña-Vázquez, P. Bermejo-Barrera.*

P033 Analysis of pollutants in water by combining ICP-AES and UV-visible spectroscopy. *J.M. Suárez-Muñoz, R. Pascual-Juez.*

P034 Analysis of ceramics decoration and coverings from the oppidum of puente tablas (Jaén, España) by MRS, XRD and XRF. *Alberto Sánchez, David-Jesús Parras, José-Alfonso Tuñón, Manuel Montejo, Peter Vandenabeele, María-Oliva Rodríguez, Carmen Rísquez.*

P035 The palette of the Pompeian artists: In situ spectroscopic analysis of raw pigments from the Naples National Archaeological Museum (MANN). *A. Giakoumaki, M. Maguregui, A. Pitarch, U. Knuutinen, S. Fdez-Ortiz de Vallejuelo, K. Castro, I. Martínez-Arkarazo, J. M. Madariaga.*

P036 The solution to the unanswered questions in cultural heritage analysis around the Raman spectroscopy spectra of $CaSO_4$-H_2O system compounds. *N. Prieto-Taboada, O. Gómez-Laserna, I. Martínez-Arkarazo, M. A. Olazabal, J. M. Madariaga.*

P037 Structural modification of cultural heritage materials produced by CW CO_2 laser. Micro-Raman and Raman imaging studies. *S. Martínez-Ramírez, L. Diaz, J.J. Camacho.*

P038 Study of the efficacy of the desalination treatment applied to an archaeological artifact affected by chorine. *Marco Veneranda, Julene Aramendia, Silvia Fdez-Ortiz de Vallejuelo, Laura García, Iñaki García, M. Neira, Kepa Castro, and Juan Manuel Madariaga.*

P039 Rapid screening of terpenes in fragrance-free cosmetics by combining headspace single-drop microextraction and micro-fluorospectrometry. *I. Costas, N. Cabaleiro, V. Romero, I. Lavilla, C. Bendicho.*

P040 Ultrasound-assisted cytosol preparation for the determination of Cd and Cu bound to metallothioneins in mussel tissue by ICP-MS. *V. Romero, M. Costas, S. Corderí, G. Sanchez, I. Lavilla, C. Bendicho.*

P041 Optical sensors for detection and continuous monitoring of VOCs during the cooking process. *J. Sanz, S. de Marcos, J. Galbán.*

P042 Reagentless fluorescent biosensor based on chemically modified glucose oxidase and Tm3+, Yb3+ doped fluorohafnate glasses. *M. del Barrio, S. de Marcos, R. Cases, V. L. Cebolla, J. Galbán.*

P043 Development of a magnetic ELISA spectrophotometric immunosensor for the determination of cocaine in biological samples. *J.C. Vidal, J.R. Bertolín, L. Bonel, L. Asturias, M.J. Arcos-Martínez, M. Alonso-Lomillo, J.R. Castillo.*

P044 Development of a magnetic ELISA spectrophotometric immunosensor for the determination of ochratoxin A (OTA) in wheat and wine. *J.R. Bertolín, L. Bonel, J.C. Vidal, J.R. Castillo.*

P045 Development of a magnetic ELISA spectrophotometric immunosensor for the determination of fumonisin B1 in cereals. *A. Ezquerra, L. Bonel, J.C. Vidal, J.R. Castillo.*

P046 Development of a magnetic ELISA spectrophotometric immunosensor for the determination of deoxynivalenol in cereals. *S. Hernandez, A. Ezquerra, L. Bonel, J.C. Vidal, J.R. Castillo.*

P047 Analytical possibilities using flavoenzymes fluorescence: Towards to a multicomponent sensor based on ChOx fluorescence. *M.P. Lapieza-Remón, I. Sanz-Vicente, J. Galbán.*

P048 Chemical sensors based on new hydrazone derivatives. *R. Losantos, J.J. Los Arcos, D. Sampedro.*

P049 Antibiotic sensing with electrochemiluminescent sensors. *M. D. Luaces, B. Diez-Buitrago, C. Pérez-Conde, A. M. Gutiérrez, A. B. Descalzo, G. Orellana, M. C. Moreno-Bondi.*

P050 Ion mobility spectrometry as a vanguard technology to assess the quality of heat transfer fluid. *L. Criado-García, R. Garrido-Delgado, L. Arce, M. Valcárcel.*

P051 Digital image-base methods as novel tools of high efficiency in quantitative analytical determinations. *A. Lopez Molinero, M. Perez García, P. Berlín Larqué.*

P102 SIA optosensor for the simultaneous espectrofluorimetric determination of mixtures of pesticides. *I. Delgado-Blanca, A. Ruiz-Medina, P. Ortega-Barrales.*

P103 Implementation of flow-through solid phase spectroscopic transduction with photochemically induced fluorescence detection: determination of clothianidin. *J. Jiménez-López, M.P. Ruiz-Barrero, P. Ortega-Barrales, A. Ruiz-Medina.*

SESIÓN DE CARTELES 2

Estructura atómica y molecular. Nanotecnología. Plasmas. Otros.

P052 Bonding properties in HNO_3.HOCl.$(H_2O)_n$ clusters. *Rafael Escribano, Pedro C. Gómez, F. Mine Balcı and Nevin Uras-Aytemiz.*

P053 Optical properties of two isomers of the heteronuclear complex $[\{Au(C_6Cl_5)_2\}Ag([9]aneS_3)]_2$. *R. Donamaria, M.C. Gimeno, V. Lippolis, J.M. Lopez-de-Luzuriaga, E. Manso, M. Monge, M.E. Olmos.*

P054 Stability of interstellar carbonaceous dust analogues and the aminoacid glycine under UV irradiation and electron bombardment. *Belén Maté, Isabel Tanarro, Miguel A. Moreno, Miguel Jiménez-Redondo, Rafael Escribano, and Víctor J. Herrero.*

P055 Electrochemical SERS spectra of isonicotic acid analyzed under a photoinduced charge-transfer mechanism. *I. López-Tocón, J. Román-Pérez, J. Soto, J.C. Otero.*

P056 Comparison of the luminescent properties of tetrahedral Au(I)-Sn(II) and Au(I)-Ge(II) complexes. *R. Echeverría, V. R. Bojan, J. M. López-de-Luzuriaga, M. Monge, M. E. Olmos.*

P057 Terpyridine Au(I) and Au(III) organometallic compounds: redox and photophysical properties. *E. Manso, J.M. Lopez-de-Luzuriaga, M. Monge, M.E. Olmos.*

P058 Self-assembly structures of 2-propil-1H-bencimidazol in solution and solid phases: A vibrational (IR, far IR, Raman and VCD) and computational study. J. *J. López-González, M. M. Quesada-Moreno, P. Cabildo, R. M. Claramunt, I. Alkorta, J. Elguero, J. R. Avilés-Moreno.*

P059 When sugars do not seem sugars, where is the carbonyl? *M. M. Quesada-Moreno, L. M. Azofra, J. R. Avilés-Moreno, I. Alkorta, J. Elguero and Juan Jesús López-González.*

P060 Molecular properties of zwitterionic, protonated and deprotonated forms of L-valine by vibrational spectroscopy (IR, Raman, VCD) and quantum chemical calculations. *J. R. Avilés-Moreno, M. M. Quesada-Moreno, A. A. Márquez-García, J. J. López-González.*

P061 Insights into the structure / vibrational spectra relationship of the system [Ca(l-Lac)(H2O)$_2$]+ from DFT, NBO and QTAIM. *A.A. Márquez García, M.C. Ramírez Avi, F. Partal Ureña.*

P062 SERS of 4-aminothiophenol (4-ATP) adsorbed on Ag and Pt nanoparticles: Photochemical transformation or chemical enhancement? *J. M. Pérez, F. J. Vidal-Iglesias, J. Solla-Gullón, J.M. Feliu.*

P063 Detailed laboratory and DFT calculated far and mid-IR spectroscopy of phyllosilicates. *V. Timón, M.A. Moreno Alba, F. Colmenero, A.M. Fernández.*

P064 Combining FTIR, Raman and INS for a full vibrational assignment of $[H_3N(CH_2)_3NH_3]^{2+}$. *Sofia R.O. Mendes, J. Tomkinson, M.P.M. Marques, L.A.E. Batista de Carvalho.*

P065 Conformational preference and spectroscopic properties of tobacco alkaloids: (-)-S-nicotine, (-)-S-cotinine and (+)-R-anabasine. Theoretical calculations and experimental insights. *P.G. Rodríguez Ortega, M. Montejo, F. Márquez, J. J. López.*

P066 Assessment of the occurrence of anomeric effect and its associated VCD spectroscopic features: A case of study. *P.G. Rodríguez Ortega, M. Montejo, F. Márquez, J. J. López.*

P067 Infrared activation of the breathing mode of methane. *M. A. Moreno, R. Escribano, O. Gálvez, V.J. Herrero, B. Maté, V. Timón.*

P068 Excited state proton transfer reactions of anti-tumor agents in cyclodextrin nanocavities. *M. A. Martín, V. Cervera-Carrascón, N. Viejo, B. Lanzón, V. González-Ruiz, A.I. Olives.*

P069 Different solvent-induced luminescent responses in Pt_2Pb clusters. *M. T. Moreno, J. R. Berenguer, E. Lalinde, A. Martín, S. Ruiz, S. Sánchez, H. R. Shashavari.*

P070 Characterization of supramolecular complexes formed between non-steroidal anti-inflammatory drugs and cucurbit[n]urils in solution and adsorbed on silver nanoparticles. *P. Sevilla, E. Corda, M. Hernández, J.V. García-Ramos, Concepción Domingo.*

P071 Determination of silver content in polymeric and inorganic nanomaterials by microwave-assisted digestion followed by flame atomic absorption spectroscopy. *A. Torrecilla, J. Crespo, J.M. López-de-Luzuriaga, M. Monge, E. Olmos, M.T. Tena, J. Villanueva.*

P072 AsFlFFF-UV-Vis-ICP-MS applied to cellular toxicity studies of silver nanoparticles: characterization of silver forms in culture media and cells. *I. Abad-Álvaro, E. Bolea, J. Jiménez-Lamana, C. Bladé, F. Laborda, J.R. Castillo.*

P073 Bioavailability of silver nanoparticles and silver speciation in biological systems through separation techniques and ICPMS detection. *J. Jiménez-Lamana, F. Laborda, E. Bolea, I. Abad, J. Bianga, M. He, K. Bierla, S. Mounicou, J.M. Rouanet, J.R. Castillo, J. Szpunar.*

P074 Multi-analytical characterization of engineered cerium oxide nanoparticles by spectroscopic techniques. *L. Sánchez-García, C. Cubel , E. Bolea , F. Laborda , J.R. Castillo.*

P075 Silver nanoparticle-proteins interaction: Evaluation of protein corona formation. *C. Villanueva , M.S. Jiménez, M.T. Gómez, J.R. Castillo.*

P076 Control of the bioconjugation of functionalized luminescent nanoparticles to antibodies by asymmetrical flow field-flow fractionation coupled to elemental and molecular spectrometry detection. *Mario Menéndez-Miranda, José M. Costa-Fernández, Jorge Ruiz Encinar and Alfredo Sanz-Medel.*

P077 In vitro evaluation of cellular uptake and toxicity of engineered L-cysteine capped phosphorescent Mn^{2+}-doped ZnS quantum dots. *E. Sotelo-González, H. Muñoz-Cimadevilla, D. Hevia, R. Sainz, J.C. Mayo, J.M. Costa-Fernández and A. Sanz-Medel.*

P078 Optical spectroscopy of metal-semiconductor nanowires: Transparent nanocontacts. *D.R. Abujetas, R. Paniagua-Domínguez, L.S. Froufe-Pérez, J.J. Sáenz, J.A. Sánchez-Gil.*

P079 Highly effective SERS nanopattern substrate. The enhancement is demonstrated using thiophenol as a molecular probe. *M.R. Lopez-Ramirez, A.R. Guerrero, J.L. Castro, J.C. Otero, R.F. Aroca.*

P080 Study in nanoscale of bivalve mollusk scallop for application as raw material in the industry. *L.R. Victorio, L. De Los Santos, A. Bustamante.*

P081 Assessing the uniformity of API distribution in low dosage pharmaceuticals using Raman spectroscopy. *D. Gómez, J. Coello, S. Maspoch.*

P082 Determination of additives from plastic polymers by focused ultrasonic solid-liquid extraction. *C. Moreta, M.T. Tena.*

P083 Formation of ABTS radical cation for antioxidant tests in the presence of silver nanoparticles as revealed by surface-enhanced raman scattering. *A. Garcia-Leis, J.V. Garcia-Ramos, Z. Jurasekova, G. Fabriciova, M. Antalik, D.Jancura and S. Sanchez-Cortes.*

P084 Monitoring vineyard parameters through at-field hyperspectral indices. *J. Aparicio, N. Sánchez, J. Martínez-Fernández, C.M. Herrero-Jiménez.*

P085 Luminescent cyclometalated Pt(II) and Pt(IV) complexes. *N. Giménez, J.R. Berenguer, J. Fernández, E. Lalinde, M. T Moreno, S. Ruiz.*

P086 Phosphors and chemiluminiscent reactions for the experimental assessment of uncertainty in fluorescence detectors. *C. Ubide, J. León, M. Ostra, M. Vidal.*

P087 Characterization of linear alcohol ethoxylates by ion mobility spectrometry. *J. Brassier, S. Armenta, M. Alcalá, M. Blanco.*

P088 Fluorescence study of GFP-chromophore analogs and their application as cell markers. *D. Martínez-López, S. Gutiérrez, M. Morón, D. Sucunza, D. Sampedro, A. Domingo, C. Burgos, J. J. Vaquero.*

P089 Nanotubes of carbon (CNTs) applications in medicine and engeneering. *C. Manteca-Diego, S. Domenech, J. Domenech.*

P090 Spectroscopy analysis of different types of impact melts: Libyan Desert glass and Darwin glass. *K. Castro, J. Aramendia, L. Gomez-Nubla, S. Fernández-Ortiz de Vallejuelo, A. Alonso-Olazabal, M.C. Zuluaga, L. A. Ortega, X. Murelaga, J.M. Madariaga.*

P091 Laser induced breakdown spectroscopy as a geochemical tool to determine paleoclimatic changes using speleothem. *A. Marín-Roldán, J. A. Cruz, J. Martín-Chivelet, M.J. Turrero, A.I. Ortega, J. O. Cáceres.*

P092 Time evolution of the infrared laser ablation plasma plume of SiO. *L. Díaz, J. J. Camacho, J. P. Cid, J.M.L. Poyato.*

P093 Spectral characterization and temporal evolution of the induced plasma emission in the ablation of aluminium alloy. *V. Oliver, J.P. Cid, S. Lago, L. Diaz, J.J. Camacho, J.M.L. Poyato.*

P094 Time characterization of the laser ablation plasma plume of CaO produced by a pulsed infrared TEA-CO_2 laser. *J.P. Cid, J.J. Camacho, L. Diaz, V.Oliver, J.M.L. Poyato.*

P095 Pulse tuneable SLM laser in the 205 nm UV region tailor-made for laser aided plasma diagnostic. *L.M. Fuentes, K. Grützmacher, C. Pérez, M.I. de la Rosa.*

P096 Ultrafast elemental mapping via pulsed radiofrequency glow discharge optical emission spectroscopy. *C. González de Vega, D. Alberts, G. Gamez, V. Chawla, G. Mohanty, I. Utke, J. Michler, R. Pereiro, N. Bordel, A. Sanz-Medel.*

P097 Development and analytical characterization of a laser ablation glow discharge optical emission spectroscopy prototype (LA-GD-OES). *C. González de Vega, C. Álvarez LLamas, N. Bordel, R. Pereiro, A. Sanz-Medel.*

P098 Simultaneous ion-photon measurements in laser-induced plasmas of organic compounds. *T. Delgado, J.M. Vadillo, J.J. Laserna.*

P099 Differential laser-matter interaction in the ablation of solid samples with laser pulses in the interval between 35 fs – 4 ps. *M. López-Claros, I.M. Carrasco, J.M. Vadillo, J.J. Laserna.*

P100 Time and space resolved optical emission diagnostics of laser induced breakdown muscle tissue samples. *J.J. Camacho, L. Diaz, S. Martinez-Ramirez, J.P. Cid, A. Marin-Roldan, S. Moncayo, J.O. Caceres.*

P101 LIPS spectroscopy for chlorine detection in cement samples. *J. Mateo, M.C. Quintero, A. Rodero.*

Optical spectroscopy of metal-semiconductor nanowires: Transparent nanocontacts

D.R. Abujetas[(1)], R. Paniagua-Domínguez[(1)], L.S. Froufe-Pérez[(1)], J.J. Sáenz[(2)], J.A. Sánchez-Gil[(1)]

(1) Instituto de Estructura de la Materia, Consejo Superior de Investigaciones Científicas (IEM- CSIC), Serrano 121, 28006 Madrid, Spain. *diego.romero@iem.cfmac.csic.es*

(2) Condensed Matter Physics Dept. and Centro de Investigación en Física de la Materia Condensada (IFIMAC), Universidad Autónoma de Madrid, Fco. Tomás y Valiente 7, 28049-Madrid, Spain.

In recent years, plasmonic cloaking has received considerable attention as a mechanism to dramatically reduce the electromagnetic scattering cross section of an object [1]. Considering available technologies, the use of metalic nanowires (NW) is suited for many optics and optoelectronics applications [2,3]. In this work [4] NWs coated with a high permittivity dielectric are proposed as means to strongly reduce the light scattering of the conducting NW (Fig. 1), rendering them transparent at infrared wavelengths of interest in optical spectroscopy. We find appropriate parameters to reduce the scattering efficiency of hybrid metal dielectric NW by up to three orders of magnitude as compared with the scattering efficiency of the homogeneous metallic NW. The bandwidth of the transparent region entirely covers the near IR telecommunications range. Although this effect is optimum at normal incidence and for a given polarization, rigorous theoretical and numerical calculations reveal that transparency is robust against changes in polarization and angle of incidence. A wealth of applications based on metal-NWs may benefit from such invisibility.

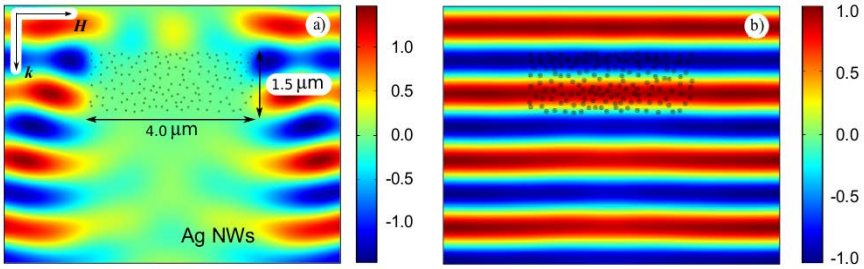

Fig. 1. (a) Map of the electric field along the cylinder axis direction at a wavelength of λ = 1550 nm for TM polarized waves for an ensemble of bare Ag Nws (R = 13.6 nm) distributed randomly within a slab of 4 μm by 1.5 μm. (b) Electric field map corresponding to the same arrangement of (a). The scattering units in this case are Ag@Si core-shell NWs (Rcore = 13.6 nm, Rshell = 45 nm), the filling fraction of the arrangement is 16%.

Acknowledgements

Spanish "Ministerio de Economía y Competitividad" (CSD2008-00066, CSD2007-00046, FIS2012-36113 and FIS2012-31070), "Comunidad de Madrid" (S2009/TIC-1476), and European Social Fund (CSIC JAE-Pre and JAE-Doc grants).

References

[1] P.-Y. Chen, J. Soric, A. Alù, Invisibility and cloaking based on scattering cancellation, Adv. Mater. **24**, (2012), OP281.

[2] Y. Li, F. Qian, J. Xiang, C. M. Lieber, Nanowire electronic and optoelectronic devices, Mater. Today **9**, (2006), 18.

[3] R. Paniagua-Domínguez, D. R. Abujetas, J. A. Sánchez-Gil, Ultra low-loss, isotropic optical negative-index metamaterial based on hybrid metal-semiconductor nanowires, Sci. Rep. **3**, (2013), 1507.

[4] R. Paniagua-Domínguez, D. R. Abujetas, L.S. Froufe-Pérez, J. J. Sáenz, and J. A. Broadband telecom transparency of semiconductor-coated metal nanowires: more transparent than glass , Opt. Express**. 21**, (2013), 22076.